Journal of Solid State Chemistry 182 (2009) 920–924

Contents lists available at ScienceDirect

Journal of Solid State Chemistry

journal homepage: www.elsevier.com/locate/jssc

Hydrothermal synthesis, crystal structure, and magnetic properties of a novel organo-templated iron(III) borophosphate: $(C_3H_{12}N_2)Fe^{III}{}_6(H_2O)_4[B_4P_8O_{32}(OH)_8]$

Ya-Xi Huang [a,b], Walter Schnelle [a], Hui Zhang [a], Horst Borrmann [a], Rüdiger Kniep [a,*]

[a] Max-Planck-Institut für Chemische Physik fester Stoffe, Nöthnitzer Straße 40, 01187 Dresden, Germany
[b] Department of Materials Science and Engineering, College of Materials, Xiamen University, 361005 Xiamen, PR China

ARTICLE INFO

Article history:
Received 2 September 2008
Received in revised form
10 January 2009
Accepted 15 January 2009
Available online 21 January 2009

Keywords:
Borophosphate
Crystal structure
Iron
Magnetic properties
Preparation

ABSTRACT

The organo-templated iron(III) borophosphate $(C_3H_{12}N_2)Fe^{III}{}_6(H_2O)_4[B_4P_8O_{32}(OH)_8]$ was prepared under mild hydrothermal conditions (at 443 K) and the crystal structure was determined from single crystal X-ray data at 295 K (monoclinic, $P2_1/c$ (No. 14), $a = 5.014(2)$ Å, $b = 9.309(2)$ Å, $c = 20.923(7)$ Å, $\beta = 110.29(2)^\circ$, $V = 915.9(5)$ Å^3, $Z = 2$, $R1 = 0.049$, $wR2 = 0.107$ for all data, 2234 observed reflections with $I > 2\sigma(I)$). The title compound contains a complex inorganic framework of borophosphate trimers $[BP_2O_8(OH)_2]^{5-}$ together with $FeO_4(OH)(H_2O)$- and $FeO_4(OH)_2$-octahedra forming channels with ten-membered ring apertures in which the diaminopropane cations are located. The magnetization measurements confirm the Fe(III)-state and show an antiferromagnetic ordering at $T_N \approx 14.0(1)$ K.

1. Introduction

Microporous materials are of great interest from both the industrial and academic point of view due to their catalytic, adsorbent, and ion-exchange properties [1–3]. The presence of large cavities in the open framework structures may provide a large internal surface area together with a large number of catalytic sites. Several investigations dealing with organically templated iron phosphates have evidenced a rich structural chemistry in these systems [4]. Following these observations we started our research on iron borophosphate including organic templates. Although many iron borophosphates without or with alkali metal/ammonium ions had been reported [5], only two organically templated iron borophosphates are known up to now: $(C_2H_{10}N_2)Fe^{II}[B_2P_3O_{12}(OH)]$ [6] and $(C_4H_{12}N_2)_3Fe^{III}{}_6(H_2O)_4[B_6P_{12}O_{50}(OH)_2]\cdot 2H_2O$ [7]. Here, we report on the hydrothermal synthesis, crystal structure, and magnetic properties of the novel organo-templated iron(III) borophosphate $(C_3H_{12}N_2)Fe^{III}{}_6(H_2O)_4[B_4P_8O_{32}(OH)_8]$, representing a templated 3D framework structure.

2. Experimental section

2.1. Synthesis

$(C_3H_{12}N_2)Fe^{III}{}_6(H_2O)_4[B_4P_8O_{32}(OH)_8]$ was prepared under mild hydrothermal conditions at 443 K. A mixture of 0.811 g $FeCl_3\cdot 6H_2O$ (Alfa, 99.8%), 1.484 g H_3BO_3 (Alfa, 99.9%), 0.822 g $C_3H_{10}N_2$ (1,3-diaminopropane, **DAP**, Aldrich, 99%) and 1.26 g H_3PO_4 (85%, Merck, p.a.) (molar ratio of 3:24:11:11), together with 7.5 ml H_2O was stirred at 333 K for 2 h. Meanwhile 0.8 ml 37% HCl was added to adjust the pH value to 1.0. The clear colourless solution was transferred into a Teflon autoclave ($V = 10$ ml, degree of filling 60–70%) and treated at 443 K for eight days. Colourless prismatic crystals of $(C_3H_{12}N_2)Fe^{III}{}_6(H_2O)_4[B_4P_8O_{32}(OH)_8]$ up to 0.2 mm in length were separated from the mother liquor by vacuum filtration followed by washing several times with deionized water and drying at 333 K in air. During our study on the preparation of the title compound, we found that the H_3BO_3 content in the starting mixture has a large effect on the final product. By keeping all the other parameters constant, the use of only half amount of H_3BO_3 (0.742 g) leads to lower yield of the title phase and an additional unidentified iron phosphate. By increasing the boron content to 2.968 g H_3BO_3, the crystal size of the title compound increases and some additional small amounts of an unknown white fine powder is observed. By this, the amount of boric acid in the starting mixture appears to be the most

* Corresponding author. Fax: +49 351 4646 3002.
E-mail address: kniep@cpfs.mpg.de (R. Kniep).

0022-4596/$ - see front matter © 2009 Elsevier Inc. All rights reserved.
doi:10.1016/j.jssc.2009.01.012

Table 1
Crystallographic data and refinement results of $(C_3H_{12}N_2)Fe^{III}_6(H_2O)_4[B_4P_8O_{32}(OH)_8]$ (e.s.d).

Molecular formula	$(C_3H_{12}N_2)Fe^{III}{}_6(H_2O)_4[B_4P_8O_{32}(OH)_8]$
Space group	Monoclinic, $P2_1/c$ (No. 14)
a (Å)	5.014(2)
b (Å)	9.309(2)
c (Å)	20.923(7)
β (deg)	110.29(2)
V (Å^3)/Z	915.9(5)/1
ρ_{calc} (g cm^{-3})	2.579
μ (Mo$K\alpha$) (mm^{-1})	2.813
Crystal size (mm^3)	$0.12 \times 0.06 \times 0.04$
Diffractometer	Rigaku R-axis RAPID, Mo$K\alpha$-radiation, Graphite monochromator
Scan type	ω-scan
2θ-range (deg)	6.0–60.0
hkl range	$-5 \leqslant h \leqslant 6$, $-13 \leqslant k \leqslant 13$, $-29 \leqslant l \leqslant 22$
R_{int}/R_σ	0.032/0.046
Measured/unique/observed ($I > 2\sigma(I)$) reflections	5837/2284/2234
Number of parameters	178
$R1/wR2$ ($I > 2\sigma(I)$)	0.048/0.107
$R1/wR2$ (all data)	0.049/0.107
Goodness-of-fit (for F^2)	1.256
Residual electron density (min/max) (e Å^{-3})	−1.233/1.735

Table 2
Atomic coordinates and equivalent/isotropic displacement parameters (Å^2) in the crystal structure of $(C_3H_{12}N_2)Fe^{III}_6(H_2O)_4[B_4P_8O_{32}(OH)_8]$ (e.s.d).

Atom	x	y	z	U_{eq}/U_{iso}
Fe1	0.40093(12)	0.68831(5)	0.78393(3)	0.00808(12)
Fe2	0.0000	0.0000	0.0000	0.00754(16)
P1	0.2184(2)	0.35277(9)	0.78970(5)	0.00746(19)
P2	0.3803(2)	0.89334(9)	0.91624(5)	0.00758(19)
B1	0.4622(9)	0.6345(4)	0.6378(2)	0.0071(7)
O1	0.4604(6)	0.5851(3)	0.70421(14)	0.0122(6)
$H1_{O1}$	0.429(14)	0.499(7)	0.707(3)	0.039(18)
O2	0.4403(6)	0.2857(3)	0.85513(14)	0.0102(5)
O3	0.1322(6)	0.8651(3)	0.94073(15)	0.0107(5)
O4	0.3400(6)	0.0474(3)	0.88445(14)	0.0111(5)
O5	0.2087(6)	0.5144(3)	0.80276(15)	0.0120(6)
O6	0.8243(7)	0.1293(3)	0.91461(15)	0.0125(6)
$H2_{O6}$	0.932(13)	0.140(6)	0.901(3)	0.025(16)
O7	0.6600(6)	0.8855(3)	0.97539(15)	0.0110(5)
O8	0.6753(6)	0.8302(3)	0.77017(14)	0.0115(5)
O9	0.3746(7)	0.7828(3)	0.86235(15)	0.0163(6)
O10	0.0687(6)	0.7846(3)	0.72135(15)	0.0145(6)
O11	0.7967(7)	0.6042(4)	0.85416(18)	0.0203(7)
$H3_{O11}$	0.895(15)	0.561(8)	0.838(4)	0.05(2)
$H4_{O11}$	0.899(19)	0.670(9)	0.875(5)	0.08(3)

Table 3
Crystal structure of $(C_3H_{12}N_2)Fe^{III}_6(H_2O)_4[B_4P_8O_{32}(OH)_8]$: selected bond lengths (Å) and angles (deg) (e.s.d).

Fe1–O9	1.906(3)	O9–Fe1–O10	93.91(13)	O5–Fe1–O1	89.84(11)
–O10	1.944(3)	O9–Fe1–O5	91.25(12)	O8–Fe1–O1	83.68(11)
–O5	1.992(3)	O10–Fe1–O5	98.48(13)	O9–Fe1–O11	84.45(14)
–O8	1.998(3)	O9–Fe1–O8	94.35(12)	O10–Fe1–O11	173.40(13)
–O1	2.034(3)	O10–Fe1–O8	94.02(13)	O5–Fe1–O11	87.95(13)
$-O11_{H2O}$	2.165(3)	O5–Fe1–O8	165.92(12)	O8–Fe1–O11	79.75(13)
		O9–Fe1–O1	175.72(14)	O1–Fe1–O11	91.44(13)
		O10–Fe1–O1	90.03(12)		
Fe2–O7	1.923(3)	O7–Fe2–O7	180.0(2)	O3–Fe2–O6	87.93(12)
–O7	1.923(3)	O7–Fe2–O3	93.42(11)	O3–Fe2–O6	92.07(12)
–O3	2.031(3)	O7–Fe2–O3	86.58(11)	O7–Fe2–O6	91.08(12)
–O3	2.031(3)	O7–Fe2–O3	86.58(11)	O7–Fe2–O6	88.92(12)
$-O6_H$	2.080(3)	O7–Fe2–O3	93.42(11)	O3–Fe2–O6	92.07(12)
$-O6_H$	2.080(3)	O3–Fe2–O3	180.00(14)	O3–Fe2–O6	87.93(12)
		O7–Fe2–O6	88.92(12)	O6–Fe2–O6	180.00(17)
		O7–Fe2–O6	91.08(12)		
P1–O10	1.516(3)	O10–P1–O5	110.55(16)	O10–P1–O2	108.42(17)
–O5	1.533(3)	O10–P1–O8	113.45(17)	O5–P1–O2	107.01(16)
–O8	1.536(3)	O5–P1–O8	108.74(15)	O8–P1–O2	108.46(16)
–O2	1.564(3)				
P2–O7	1.517(3)	O7–P2–O9	110.29(17)	O7–P2–O4	109.76(16)
–O9	1.520(3)	O7–P2–O3	110.43(16)	O9–P2–O4	109.83(17)
–O3	1.524(3)	O9–P2–O3	108.98(17)	O3–P2–O4	107.50(15)
–O4	1.564(3)				
$B1–O1_H$	1.467(5)	O1–B1–O6	111.7(3)	O1–B1–O2	108.3(3)
$-O6_H$	1.475(6)	O1–B1–O4	110.6(3)	O6–B1–O2	108.0(3)
–O4	1.476(5)	O6–B1–O4	109.6(3)	O4–B1–O2	108.6(3)
–O2	1.480(4)				
O1–H1	0.82(7)	O11–H3	0.79(8)		
O6–H2	0.70(6)	O11–H4	0.82(9)		
N1–C3	1.519(9)	N1–C3–C1	124.1(10)		
N2–C2	1.47(2)	C3–C1–C2	100.0(12)		
C1–C2	1.518(10)	C1–C2–N2	77.1(16)		
C1–C3	1.30(2)				

important factor to obtain a pure reaction product. The phase purity of samples applied for further properties investigations was checked by elemental analyses and powder X-ray diffraction.

2.2. Crystal structure determination

A colourless prismatic single crystal of $(C_3H_{12}N_2)Fe^{III}{}_6(H_2O)_4[B_4P_8O_{32}(OH)_8]$ ($0.12 \times 0.06 \times 0.04$ mm^3) was fixed on a glass fibre with two-component glue. X-ray data were collected at 295 K using a RIGAKU R-Axis RAPID diffractometer, equipped with curved R-axis Rapid imaging plate detector and a three-circle goniometer (Mo$K\alpha$ radiation, graphite monochromator). Intensity data were collected in the angular range $2.42^\circ \leqslant 2\theta \leqslant 73.82^\circ$. The data were corrected for Lorentz and polarization effects. A multi-scan absorption correction was applied. The structure was solved by direct methods in the space group $P2_1/c$ (No. 14) using the program SHELXS-97-2 [8]. Fourier calculations and subsequent full-matrix least-squares refinements were carried out by using SHELXL-97-2 [9], applying neutral atom scattering factors. The framework atom positions were all located and refined. After including anisotropic displacement parameters in the refinement, the hydrogen atoms bonded to oxygen could be located from difference Fourier maps and were refined without any restraints. The template atom positions (C and N) could not be directly located from difference Fourier maps, the procedure of how to identify them is described below. Details of the data collection and relevant crystallographic data are summarized in Table 1.[1] Atomic positions and displacement parameters for $(C_3H_{12}N_2)Fe^{III}{}_6(H_2O)_4[B_4P_8O_{32}(OH)_8]$ are given in Table 2, selected bond lengths and angles in Table 3, respectively.

The electron density of the $(C_3H_{12}N_2)^{2+}$ ions in Fourier maps (see Supporting information) clearly shows that it represents a continuous distribution which indicates a disorder of the $(C_3H_{12}N_2)^{2+}$ ions. Based on the results of the chemical analyses (see below) showing that only one $(C_3H_{12}N_2)^{2+}$ ion contributes to the formula unit, we tried to locate the C and N atoms by constraining their occupancies. The final results are shown in Fig. 1. Both C and N atom positions are only partially occupied. The organic molecules are present in two different orientations related by a centre of symmetry. Due to the overlap of the DAP molecules in a way that N1 is shared by two different orientations of the

[1] Crystallographic data (excluding structure factors) for the structure(s) reported in this paper have been deposited with the Cambridge Crystallographic Data Centre as supplementary publication no. CCDC-715705. Copies of the data can be obtained free of charge on application to CCDC, 12 Union Road, Cambridge CB2 1EZ, UK (fax: (44) 1223 336-033; e-mail: deposit@ccdc.cam.ac.uk).

same molecule, the DAP cations appear to be continuously arranged inside the framework-channels running along [001].

2.3. Characterization

The chemical composition of the title compound was confirmed by elemental analysis. Iron, boron and phosphorus were analysed using ICP-OES (VARIAN Vista); a hot extraction method was applied for organic carbon, nitrogen and hydrogen (LECO CHNS-932). The results of chemical analyses are given in wt%, *obs.*(esd)/*calc.*: Fe: 23.18(7)/23.14; B: 2.97(3)/3.04; P: 17.28(8)/17.42; C: 2.472(5)/2.533; N: 1.835(6)/1.970; H: 2.056(4)/1.984. The results give a molar ratio of Fe:B:P:C:N = 6.04:4:8.12:3.00:1.91 which reveals only one $(C_3H_{12}N_2)^{2+}$ ion per formula unit.

Thermal investigations (DTA/TG) were carried out in a static air atmosphere with heating rates of 5 K/min up to 1073 K (NETZSCH STA 409). The TG curve of $(C_3H_{12}N_2)Fe^{III}{}_6(H_2O)_4[B_4P_8O_{32}(OH)_8]$ shows a four-step weight loss with an overall weight loss of 16.8 wt% (16.6 wt% calc., according to a hypothetical weight loss of $1 \times C_3H_{10}N_2$ and $9 \times H_2O$ per formula unit). The DTA curve reveals two endothermic peaks and three exothermic peaks with maximum temperatures at 533, 586, and 638, 759, and 842 K, respectively, accompanied by three exothermal shoulders at 618, 732, and 812 K. The thermal effects in the DTA curve are correlated to the decomposition process.

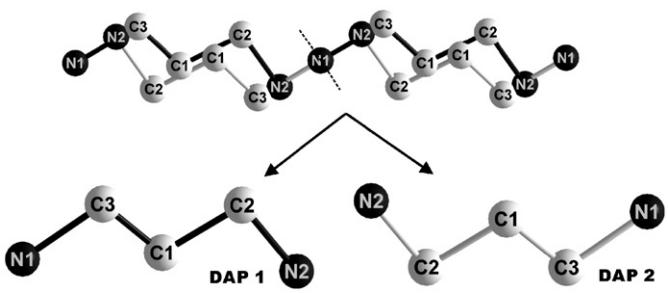

Fig. 1. The arrangement of the (disordered) 1,3-diaminopropane (DAP) cations in the crystal structure of $(C_3H_{12}N_2)Fe^{III}{}_6(H_2O)_4[B_4P_8O_{32}(OH)_8]$ shows two different orientations related by a centre of symmetry. Resulting continuous *zig-zag* arrangement (*top*), two different orientations of $(C_3H_{12}N_2)^{2+}$ ions (*bottom*).

3. Results and discussion

3.1. Crystal structure

The crystal structure of $(C_3H_{12}N_2)Fe^{III}{}_6[B_4P_8O_{32}(OH)_8]$ contains a complex inorganic framework consisting of borophosphate trimers, $[BP_2O_8(OH)_2]^{5-}$, and iron(III) octahedra arranged to form channels with ten-membered ring apertures in which the organic diaminopropane cations are located (Fig. 2(a)). The crystal structure can be disassembled into iron(III) borophosphate layers extending parallel (001) in which $FeO_4(OH)(H_2O)$ coordination octahedra interconnect the borophosphate anions (Fig. 2(b)). The layers are interlinked along [001] via $FeO_4(OH)_2$ coordination octahedra.

The borophosphate anions present the oligomeric trimers, $[BP_2O_8(OH)_2]^{5-}$, which are built from a central $BO_2(OH)_2$ tetrahedron branched by two PO_4 tetrahedra via non-protonated oxygen (Fig. 2(c)). This kind of building unit is often observed in M^{III}-borophosphates (M^{III} = Al, V, Fe, Ga, In) [5a,10,11] and in a great number of compounds containing V(IV)-heteropolyoxoanions where the borophosphate trimers are interconnected by V_2O_8 units (dimers of square pyramids) forming cyclic clusters $[(VO)2BP_2O_{10}]_m^{3-}$ ($m = 4$, 5, 6) or ribbons [12], e.g., in $NaFe[BP_2O_7(OH)_3]$ [5a], $CsV_3(H_2O)_2[B_2P_4O_{16}(OH)_4]$ [10], and $Na_{14}[Na\supset\{(VO)_2BP_2O_{10}\}_5]\cdot nH_2O$ [12b], respectively. The B–O and P–O bond lengths within the borophosphate oligomers (B–O: 1.467–1.480 Å, P–O: 1.516–1.564 Å) as well as the O–B–O and O–P–O angles (O–B–O 108.0–111.7°, O–P–O 107.01–113.45°) are in the same range as observed in the crystal structure of $NaFe[BP_2O_7(OH)_3]$ [5a]. Further details on bond lengths and angles are given in Table 3. The bond lengths within the Fe(III) coordination octahedra represent typical values for coordinative Fe(III)–O bonds [7]. The long distance of Fe(1)–O(11) (2.165 Å) is due to the aqua ligand.

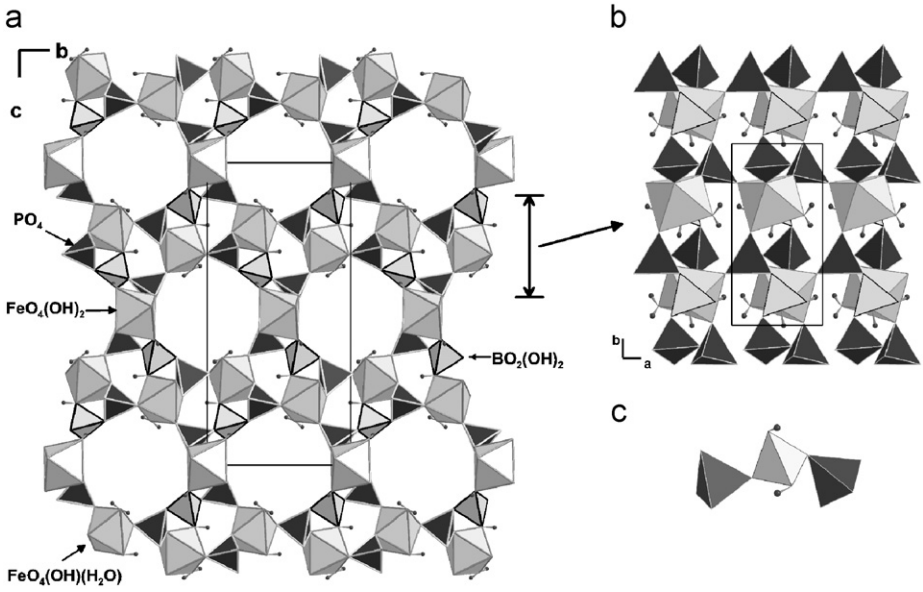

Fig. 2. (a) Polyhedral presentation of the crystal structure of $(C_3H_{12}N_2)Fe^{III}{}_6(H_2O)_4[B_4P_8O_{32}(OH)_8]$ viewed along [100], and showing the ten-membered ring channels; (b) Fe(1)-borophosphate layer viewed along [001]; (c) Oligomeric trimer $[BP_2O_8(OH)_2]^{5-}$. FeO_6 octahedra: light grey; PO_4 tetrahedra: dark grey; BO_4 tetrahedra: light grey. H atoms: small dark grey spheres. DAP species are omitted for clarity.

The 1D channels running along [100] are constructed from ten-membered rings with the topological sequence of the centres of the polyhedra given by Fe(2)–B–P–Fe(1)–P–Fe(2)–B–P–Fe(1)–P. As shown in Fig. 3 the aperture size of the channel is around $7.69 \times 9.26\,\text{Å}^2$ (O6 · · · O6 and O5 · · · O5) (Fig. 3). The channels run parallel [100] and exhibit the motif of a hexagonal rod packing. The DAP cations are located in the centre of the channels with their long axis ($d_{\text{N}\cdots\text{N}} = 4.93\,\text{Å}$) parallel to the channel. The combination of the large aperture of the channel together with the coinciding orientation of the long axis of the template and the central axis of the channel gives already a hint for only weak interactions between template and host resulting in the disorder of the DAP cations. In general, framework atoms interacting with a template (e.g. via hydrogen bonds) are also influenced by a disorder of the template species. In the title compound, however, the framework atom positions can be refined to a rigid model without any problems and even the hydrogen atoms bonded to oxygen are refined with proper thermal parameters without any restraints. The only weak interactions between framework and template cations suggest the chance for ion exchange reactions.

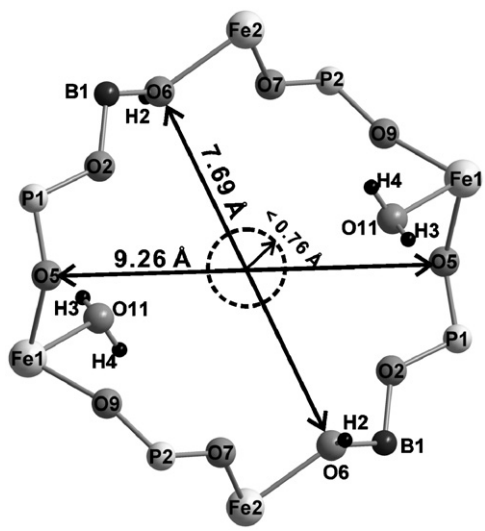

Fig. 3. Ball-and-stick presentation of a ten-membered ring with an aperture size of $7.69 \times 9.26\,\text{Å}^2$ (O2 · · · O2 and O5 · · · O5), the central circle part represent the area where the 1,3-diaminopropane cations are located (the area does not include hydrogen).

A very close structural resemblance to $(C_3H_{12}N_2)Fe^{III}{}_6(H_2O)_4[B_4P_8O_{32}(OH)_8]$ is given by $CsV_3(H_2O)_2[B_2P_4O_{16}(OH)_4]$ [10], which is also made up of two crystallographically different metal-oxygen coordination octahedra linked by borophosphate trimers. Their framework structures, however, show a different arrangement (Fig. 4) with the main difference in size and shape of channels: The vanadium compound contains elliptic channels built from eight-membered rings (Fig. 4(a)), whereas in case of the title compound the more tube-like channels are constructed from ten-membered rings with a larger aperture size because of the two additional coordination octahedra. As can also be seen from Fig. 4 the vanadium compound contains additional channels characterized by an aperture formed from six-membered rings whereas the additional channels in the iron compound show a smaller aperture formed by five-membered rings.

3.2. Magnetic measurements

The magnetization measurements of $(C_3H_{12}N_2)Fe^{III}{}_6(H_2O)_4[B_4P_8O_{32}(OH)_8]$ were performed on a SQUID-magnetometer (Quantum Design, MPMS XL-7) in the temperature range 1.8–400 K in various external magnetic fields. For temperatures above the phase transition temperature (see below) the inverse magnetic susceptibility $1/\chi = H/M$ versus temperature T is independent of field H. For $T > 50$ K the data for $H = 1$ kOe (Fig. 5) can be described by a Curie–Weiss law. Taking into account the diamagnetic increments according to Pascal's method for DAP [13] and according to Klemm for the ionic part [13] (total $\chi_{\text{dia}} = -541 \times 10^{-6}$ emu/mol) an effective magnetic moment of $\mu_{\text{eff}} = 5.95\mu_{\text{B}}$ per Fe-atom was obtained by a non-linear fit of $\chi(T)$. The resulting Weiss constant is $\theta = -56.1$ K. A linear fit to $1/(\chi - \chi_{\text{dia}})$ in the same temperature range yielded similar values ($\mu_{\text{eff}} = 5.89\mu_{\text{B}}$ per Fe-atom, $\theta = -52.2$ K). μ_{eff} is in good agreement with typical values for octahedrally coordinated high-spin Fe^{III}-ions while the large negative Weiss constant θ indicates strong antiferromagnetic interactions between the moments. The deviations from the Curie–Weiss law observed at low temperatures are shown in the inset of Fig. 5. A spontaneous magnetization is visible, especially at weaker fields. The spontaneous moment is only around $0.10\mu_{\text{B}}$ per formula unit. Such a low ordered moment is typical for a weak ferromagnet. Here, a ferromagnetic component exists in a basically antiferromagnetic arrangement of the Fe 3*d*-moments, which probably originates from a small canting of the moments. The magnetic ordering is observed at $T_{\text{N}} \approx 14.0(1)$ K.

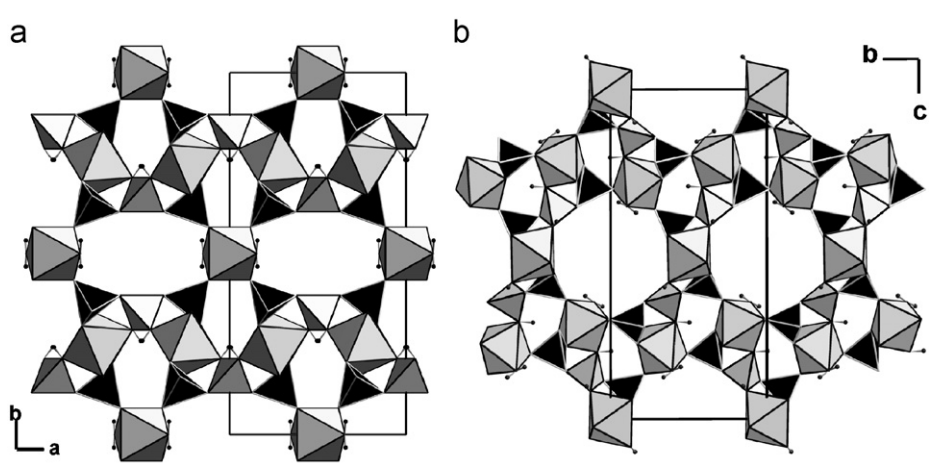

Fig. 4. Comparison of the framework arrangement in the crystal structures of $CsV_3(H_2O)_2[B_2P_4O_{16}(OH)_4]$ [11] and $(C_3H_{12}N_2)Fe^{III}{}_6(H_2O)_4[B_4P_8O_{32}(OH)_8]$. Eight-membered ring channels are represent in the V-compound (a) whereas ten-membered ring channels are formed in the Fe-compound (b). FeO_6/VO_6 octahedra: light grey; PO_4 tetrahedra: dark grey; BO_4 tetrahedra: light grey. H atoms: small dark grey spheres. Cs and DAP are omitted for clarity.

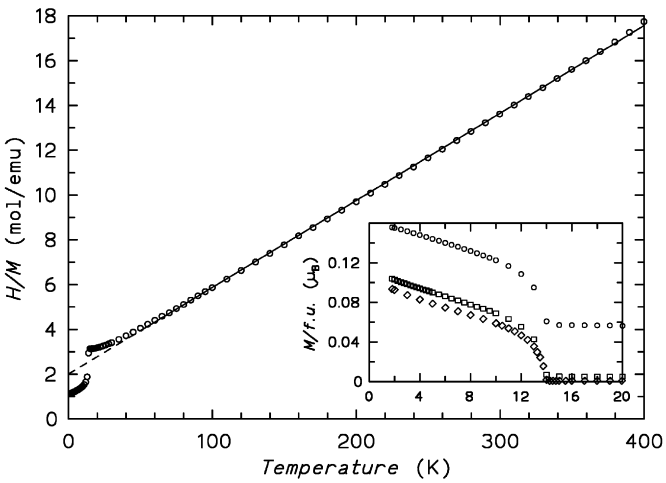

Fig. 5. Magnetic properties of $(C_3H_{12}N_2)Fe^{III}{}_6(H_2O)_4[B_4P_8O_{32}(OH)_8]$: inverse molar magnetic susceptibility $1/\chi = H/M$ for $H = 1$ kOe against temperature. The line shows the linear Curie–Weiss fit (see text). Inset: field-cooling magnetization $M(T)$ in different external fields (from top to bottom: 1000 Oe (circles), 100 Oe (squares), 20 Oe (diamonds)).

4. Conclusion

The crystal structure of $(C_3H_{12}N_2)Fe^{III}{}_6(H_2O)_4[B_4P_8O_{32}(OH)_8]$ contains a complex inorganic framework of borophosphate trimers $[BP_2O_8(OH)_2]^{5-}$ and iron(III) octahedra arranged around channels which are formed with ten-membered ring apertures in which the organic diaminopropane cations are located. The incorporation of diaminopropane cations extends the known iron borophosphate framework into the large pore size range and at the same time shows that the crystal structures of microporous borophosphates are very sensitive to the nature of the templates. When piperazine is used instead of diaminopropane, a different structure with chemical composition $(C_4H_{12}N_2)_3Fe^{III}{}_6(H_2O)_4[B_6P_{12}O_{50}(OH)_2]\cdot 2H_2O$ [6] is formed. Magnetic measurements on the title compound indicate the existence of an antiferromagnetic ordering at low temperatures.

Acknowledgments

This work was supported by the Fonds der Chemischen Industrie. The authors would like to thank Dr. G. Auffermann and Mrs. A. Völzke for chemical analyses (ICP-OES) as well as Dr. R. Niewa and Ms. S. Müller for thermal investigations.

Appendix A. Supplementary material

The online version of this article contains additional supplementary data. Please visit doi:10.1016/j.jssc.2009.01.012.

References

[1] A.K. Cheetham, G. Férey, T. Loiseau, Angew. Chem. Int. Ed. 38 (1999) 3268–3292.
[2] D.W. Breck, Zeolite Molecule Sieves: Structure, Chemistry and Use, Wiley, New York, 1974.
[3] S. Gao, J.B. Moffat, J. Catal. 180 (1998) 142–148.
[4] K.-H. Lii, Y.-F. Huang, V. Zima, C.-Y. Huang, H.-M. Lin, Y.-C. Jiang, F.-L. Liao, S.-L. Wang, Chem. Mater. 10 (1998) 2599–2609 and the references therein.
[5] (a) I. Boy, G. Cordier, B. Eisenmann, R. Kniep, Z. Naturforsch. 53b (1998) 165–170;
(b) I. Boy, C. Hauf, R. Kniep, Z. Naturforsch. 53b (1998) 631–633;
(c) R. Kniep, I. Boy, H. Engelhardt, Z. Anorg. Allg. Chem. 625 (1999) 1512–1516;
(d) H. Engelhardt, R. Kniep, Z. Kristallogr, NCS 214 (1999) 443–444;
(e) R. Kniep, H.G. Will, I. Boy, C. Röhr, Angew. Chem. Int. Ed. Engl. 36 (1997) 1013–1014;
(f) A. Yilmaz, X. Bu, M. Kizilyalli, G.D. Stucky, Chem. Mater. 12 (2000) 3243–3245;
(g) Y.-X. Huang, G. Schäfer, W. Carrillo-Cabrera, R. Cardoso, W. Schnelle, J.-T. Zhao, R. Kniep, Chem. Mater. 13 (2001) 4348–4354;
(h) M. Kritikos, E. Wikstad, K. Walldén, Solid State Sci. 3 (2001) 649–658;
(i) T. Yang, G. Li, J. Ju, F. Liao, M. Xiong, J. Lin, J. Solid State Chem. 179 (2006) 2534–2540;
(j) Y.-X. Huang, B. Ewald, W. Schnelle, Yu. Prots, R. Kniep, Inorg. Chem. 45 (2006) 7578–7580.
[6] R. Kniep, G. Schäfer, Z. Anorg. Allg. Chem. 626 (2000) 141–147.
[7] Y.-X. Huang, Yu. Prots, W. Schnelle, R. Kniep, Sci. Technol. Adv. Mater. 8 (2007) 399–405.
[8] G.M. Sheldrick, SHELXS 97-2, Program for the Solution of Crystal Structures, Göttingen, 1997.
[9] G.M. Sheldrick, SHELXL 97-2, Program for Crystal Structure Refinement, Göttingen, 1997.
[10] H. Engelhardt, H. Borrmann, W. Schnelle, R. Kniep, Z. Anorg. Allg. Chem. 626 (2000) 1647–1652.
[11] (a) D. Koch, R. Kniep, Z. Kristallogr. NCS 214 (1999) 441–442;
(b) Y.-X. Huang, S.-Y. Mao, J.-X. Mi, Z.-B. Wei, J.-T. Zhao, R. Kniep, Z. Kristallogr. NCS 216 (2001) 15–16;
(c) Y.-X. Huang, J.-X. Mi, S.-Y. Mao, Z.-B. Wei, J.-T. Zhao, R. Kniep, Z. Kristallogr. NCS 217 (2002) 7–8;
(d) J.-X. Mi, Y.-X. Huang, S.-Y. Mao, H. Borrmann, J.-T. Zhao, R. Kniep, Z. Kristallogr. NCS 217 (2002) 167–168;
(e) L. Zhang, H. Zhang, H. Borrmann, R. Kniep, Z. Kristallogr. NCS 217 (2002) 447–448.
[12] (a) C.J. Warren, R.C. Haushalter, D.J. Rose, J. Zubieta, Chem. Mater. 9 (1997) 2694–2696;
(b) R.P. Bontchev, J. Do, A.J. Jacobson, Angew. Chem. Int. Ed. 38 (1999) 1937–1940;
(c) J. Do, L.-M. Zheng, R.P. Bontchev, A.J. Jacobson, Solid State Sci. 2 (2000) 343–351;
(d) J. Do, R.P. Bontchev, A.J. Jacobson, Inorg. Chem. 39 (2000) 4305–4310;
(e) Y. Zhao, Z. Shi, S. Ding, N. Bai, W. Liu, Y. Zou, G. Zhu, P. Zhang, Z. Mai, W. Pang, Chem. Mater. 12 (2000) 2550–2556.
[13] E. König, G. König, in: Landolt-Börnstein, New Series 12/4a, Springer, Berlin, 1984.